Proceedings of the Combustion Institute 41 (2025) 105912

Contents lists available at ScienceDirect

Proceedings of the Combustion Institute

journal homepage: www.elsevier.com/locate/proci

A semi-detailed pyrolytic gas-phase kinetic model for the volatiles of polyethylene thermal degradation

Andrea Locaspi [a,1], Alessandro Pegurri [a,1], Marco Mehl [a], Matteo Pelucchi [a], Sittichai Natesakhawat [b,c], Hang Zhou [d,e], Yupeng Xu [d,e], Ping Wang [b], Mehrdad Shahnam [d], Tiziano Faravelli [a,*]

[a] Department of Chemistry, Materials, and Chemical Engineering "G. Natta", Politecnico di Milano, Piazza Leonardo da Vinci 32, 20133, Milano, IT
[b] National Energy Technology Laboratory, 626 Cochran Mill Road, Pittsburgh, PA 15236, USA
[c] National Energy Technology Laboratory Support Contractor, 626 Cochran Mill Road, Pittsburgh, PA 15236, USA
[d] National Energy Technology Laboratory, 3610 Collins Ferry Road, Morgantown, WV 26505, USA
[e] National Energy Technology Laboratory Support Contractor, 3610 Collins Ferry Road, Morgantown, WV 26505, USA

ARTICLE INFO

Keywords:
Polyethylene
Kinetics
Pyrolysis
Plastic waste
Gas-phase reactions

ABSTRACT

In a circular economy approach, plastic waste is a source of valuable chemicals and energy vectors. Thermochemical technologies such as pyrolysis, gasification, and combustion enable the valorization of even complex and contaminated waste streams. While condensed-phase degradation governs overall reactivity, accurately modeling the gas-phase reactivity of pyrolysis products is essential for scaling up valorization processes in industrial reactors. Isolating the pyrolysis behavior of volatiles first allows the decoupling of complexities associated with the low-temperature oxygen reactivity. This work presents a semi-detailed kinetic model to address the pyrolytic gas-phase reactivity of volatiles formed during the thermal degradation of polyethylene (PE). The model builds on a validated multi-step condensed-phase kinetic model and employs established lumping approaches. Short-chain compounds are modeled with high detail, while long-chain ones are described by surrogate species representative of diesel-cuts ($NC_{16}H_{32}$) and waxes ($NC_{30}H_{60}$). The reactivity of short chains is described through the comprehensive CRECK kinetic model by incorporating recent experimental data to refine reaction pathways of C_5—C_7 olefins. Due to the lack of experimental data for longer olefins, their reactivity is modeled by analogy to the shorter ones, ensuring an asymptotic behavior with increasing carbon numbers. The semi-detailed model is validated against experimental data on PE pyrolysis, assuming instantaneous mixing of the inert inlet flow with released volatiles, followed by a segregated plug-flow behavior. Validation across different reactor setups confirms the model's capability to predict detailed product distributions. Despite minor discrepancies, the proposed model effectively captures experimental trends. Future work will address modeling the reactivity in oxygen-containing environments.

1. Introduction

Chemical recycling and waste valorization processes are key to a sustainable chemical industry, circular economy, and carbon management [1]. Pyrolysis, combustion, and gasification technologies enable the conversion of complex feedstocks such as plastic wastes (PW) and municipal solid wastes (MSW) [2]. Product distribution optimization, design of experiments, reactors, and processes, and control of pollutant formation can largely benefit from fluid dynamics and chemical kinetic modeling tools.

While studies on PW combustion and gasification are recent [3], studies on the chemical kinetics of condensed-phase degradation of pure polyolefins date back to the late 1990s [4,5], as it represents the initial step before secondary pyrolysis, gasification, and oxidation of the released products. Several kinetic models of varying complexities have been proposed for polyethylene (PE) pyrolysis. The simplest ones are global models, obtained from fitting single experiments [6,7], but they do not differentiate among gas and condensed-phase reactions leading

* Corresponding author.
E-mail address: tiziano.faravelli@polimi.it (T. Faravelli).
[1] These authors contributed equally to this work.

https://doi.org/10.1016/j.proci.2025.105912
Received 30 April 2025; Accepted 26 September 2025
Available online 11 October 2025
1540-7489/© 2025 The Authors. Published by Elsevier Inc. on behalf of The Combustion Institute. This is an open access article under the CC BY license (http://creativecommons.org/licenses/by/4.0/).

to case-specific predictions. Conversely, physics-based models offer higher detail but are currently limited to the condensed-phase reactivity [8–11]. Accurate gas-phase description is crucial for modeling industrial reactors, where high temperatures and long residence times enhance light gas formation, aromatics, and soot, and result in interactions between degradation products from different polymers. Semi-detailed models offer a practical balance between detail and computational cost to study complex reactors [12]. Although gas-phase chemistry has been widely studied, the reactivity of volatiles from polymer degradation has been explored only very recently [13]. For PE, the primary volatiles include C_2H_4 and oligomers [9], encompassing linear paraffins, 1-olefins, and α-ω-diolefins from C_2 to C_{40+}. While normal paraffin reactivity has been widely explored [14–17], kinetic models are publicly available only for olefins up to C_7 [18–22].

The present work proposes a semi-detailed kinetic model to describe the secondary pyrolytic reactivity of volatiles released from PE thermal degradation, complementing a recently published multi-step condensed-phase model [9]. The model builds on the core mechanism of the CRECK gas-phase model [23], updating the C_5–C_7 olefins pyrolytic reactivity based on recent speciation data [19–21,24,25], and introducing the reactivity of long chain olefins released from the condensed-phase model. The latter is described by analogy to shorter olefins and employing validated lumping techniques [12,26]. The resulting model is validated against literature experimental data on C_5–C_7 olefins and high-temperature PE pyrolysis, demonstrating its ability to predict key products over a wide range of operating conditions. To the best of the authors' knowledge, this is the first physics-based model for PE thermal degradation. Future work will expand the proposed model to account also for the reactivity in O_2-containing environments. Coupling this model with similar ones for other polymers [9,27,28] enables a comprehensive and consistent description of thermochemical valorization of complex wastes or industrial applications such as solid propellants.

2. Kinetic model

The model describes the gas-phase reactivity of volatiles formed from PE condensed-phase pyrolysis. The aim is to describe, at a low computational cost, the major products released by varying reactor temperature, pressure and gas-phase residence time. The thermochemistry of long-chain olefins is defined by group contribution methods [9], while transport properties are estimated as outlined by Holley et al. [29], where critical properties are obtained by method of Nanoolal [30]. The CHEMKIN-format kinetic model is attached as Supplementary Material (SM) and is also freely available on GitHub [23].

2.1. Species definition

This mechanism builds on a validated condensed-phase multi-step model for PE thermal degradation [9]. In this framework, the plastic material is represented by two species corresponding to crystalline and amorphous polymer fragments, identified by the "P-" in their labels. Conversely, volatiles are described through real species employing largely validated lumping techniques for pyrolysis and combustion models [12,26]. These volatiles are permanent gases (C_2H_4, C_3H_8, C_3H_6, C_4H_6), the trimer (NC_6H_{12}), and long-chain olefins representative of diesel-cuts ($NC_{16}H_{32}$) and waxes ($NC_{30}H_{60}$). The reactivity of short-chain compounds is described by the CRECK kinetic model [31,32], also accounting for formation of polyaromatics, and includes 150 species and 3268 reactions. The reactivity of C_{5+} is discussed in the next section and introduces 1 species and 58 reactions per olefin, with 54 out of 58 reactions being H-abstractions, for a total of 5 olefin species and 290 reactions. The overall PE model considers 2 liquid-phase species, 10 liquid-phase reactions, 155 gas-phase species, and 3558 gas-phase reactions.

2.2. Reaction mechanism of C_{5+} 1-Olefins

The reactivity of all olefins is developed systematically employing rate rules first validated on C_5–C_7 olefins. The reaction mechanism follows radical degradation pathways, where the considered species decompose through initiation, propagation, and termination reactions. Retro-ene reactions are also considered, although they have a lower impact under the conditions of interest.

To reduce the computational cost, the reaction mechanism is formulated without introducing diolefins. While polyolefin pyrolysis forms paraffins, olefins, and diolefins, the overall H/C ratio and functional group reactivity of the products can be adequately represented using only olefins [9]. Another key simplification is achieved by neglecting long-chain radicals [33]. Due to the low gas-phase concentrations, radicals formed under pyrolytic conditions fully decompose by unimolecular pathways, as H-abstractions are ~10–100 times slower under typical operating conditions [26]. The products of these reactions are shorter olefins described through the lever rule [34], and short-chain radicals that are modeled with a higher level of detail by the core mechanism. This approach allows neglecting radicals of long-chain olefins, it does not affect the predicted total radical concentration, as all reactions preserve the correct radical balances, and proves reliable across the temperature and pressure range typical of PW thermochemical recycling. Conversely, this limits the model applicability for O_2-containing environments, where the oxygen addition to alkenyl radicals is competitive with β-scission [35]. Considering n-heptane, which has higher low temperature reactivity than olefins, NTC behavior of ignition delay times is not observed in air at atmospheric pressure while they become important at $T < 700$ °C for $P = 10$ bar and $T < 800$ °C for $P = 100$ bar [12]. These operating conditions are outside the range of interest for PW gasification [3], but may be relevant to predict low temperature ignition in fire safety studies. For these conditions, this methodology can be updated by introducing the corresponding long-chain alkyl radicals and the peroxide intermediates, although at a higher computational cost.

The long-chain radicals are assumed to decompose analogously to the condensed-phase model: internal radicals undergo β-scission to form terminal ones, which in turn unzip to C_2H_4 or undertake 1–5 isomerization followed by β-scission to release NC_6H_{12} as resulting from the radical transfer reaction. Both reactions form a terminal radical which can again decompose until the formation of short chain radicals. 1–4, 1–6, and multiple isomerizations are implicitly accounted through formation of NC_6H_{12}. Considering literature rate values [35,36] for unzipping and 1–5 isomerization, at 700 °C the latter is approximately two times faster. The selectivity between the different pathways is considered through the stoichiometric coefficients at the reference temperature of 700 °C. In principle, isomerization to form allylic radicals, cyclization reactions to form naphthenes or isoolefins, and radical additions on the double bonds should be included as well. Nevertheless, as shown in the next sections and by comparison with more detailed models [13], the proposed approach is quite accurate in predicting the product spectra of C_5–C_7 olefins.

Initiation reactions are described following this methodology. Because of the different short-chain radical products, three types of initiation reactions are considered for each olefin: allyl position, even positions, and odd positions. The first accounts for the higher radical pool compared to paraffins, and it forms an allyl radical (C_3H_5-A) and a long-chain terminal one, which, as mentioned before, is represented by its main decomposition products through a lumped reaction. For instance, considering allylic initiation on $NC_{16}H_{32}$, the reaction products should be C_3H_5-A and $NC_{13}H_{27}$, but the latter is represented as a combination of C_2H_4 and NC_6H_{12} through the following reaction:

$$NC_{16}H_{32} => C_3H_5 - A + C_2H_4 + 1.33NC_6H_{12} + NC_3H_7$$
$$k = 0.8 \times 10^{16} \times \exp(-71000/RT)$$

where NC_3H_7 is the small-chain radical obtained by the complete degradation of the long-chain species. The rate parameters are derived by analogy with previous studies [35], and align with values in literature [19,20,36]. The remaining two initiation classes lump all reactions at even and odd aliphatic positions, e.g., even-position initiation in even olefins form C_2H_5 and 1–4C_4H_7, while odd-position initiation forms NC_3H_7 and C_3H_5-A. Odd initiations employ the same stoichiometry as allylic ones, while even ones have different reaction products. Aliphatic initiation rates are obtained multiplying the per-site rate [19–21,35,36] by the number of elementary acts.

The main fuel decomposition pathways are H-abstraction reactions followed by isomerization and/or β-scissions of the fuel radicals. Due to the low gas-phase concentrations, H-abstractions are assumed to be rate determining while the released degradation products depend on the competition between isomerization and decomposition steps. The present work introduces two H-abstraction reactions representing all radical isomers, distinguishing only between allyl and alkyl positions. The former results in the formation of an allylic radical that decomposes to C_4H_6 and a terminal radical represented similarly to initiation reactions. With respect to alkyl positions, all internal secondary steps are lumped into a single step following the approach described by Ranzi et al. [26]. Specifically, the products formed from β-scissions of all internal radical sites are written separately, and then appropriately weighted in a single reaction. Only scissions to form stable olefins and alkenyl radicals are considered to avoid introducing diolefin compounds, except for radicals on the fourth carbon site as it can only decompose to form 1–5 pentadiene (LC_5H_8), an important soot precursor. All other products are represented as previously discussed. Specifically, stable olefins are modeled through the lever rule, while terminal radicals are assumed to fully decompose to short-chain radicals. For instance, a single H-abstraction reaction on all secondary hydrogens of $NC_{16}H_{32}$ is written for any abstractor radical R (e.g., CH_3, C_2H_5, NC_3H_7, C_6H_5) as:

$$\begin{aligned} R + \mathrm{NC_{16}H_{32}} \Rightarrow\ & \mathrm{RH} + 0.077\mathrm{CH_3} + 0.077\mathrm{LC_5H_8} \\ & + 0.46\mathrm{C_3H_5} - A + 0.46\mathrm{C_4H_7}1 - 4 + 1.36\mathrm{C_2H_4} \\ & + 0.55\mathrm{NC_6H_{12}} + 0.36\mathrm{NC_7H_{14}} + 0.18\mathrm{NC_{16}H_{32}} \\ & + 0.08\mathrm{NC_5H_{10}} + 0.08\mathrm{C_4H_8} - 1 + 0.08\mathrm{C_3H_6} \end{aligned}$$

The rates of abstractions are the same employed in the core CRECK kinetic model [31], scaling the frequency factor by the number of hydrogens.

Retro-ene reactions are also considered, releasing C_3H_6 and a shorter olefin described through the lever rule, considering rate parameters from the theoretical study of Popelier et al. [37]. However, these reactions have little impact on products distribution at the considered temperatures and pressures.

3. Simulation methods

The proposed kinetic model is validated with literature data on pure olefins and polyethylene pyrolysis, employing OpenSMOKE++ as simulation tool [38]. C_5—C_7 olefin validation target is addressed through appropriate ideal reactors simulations (e.g., flow reactors, …), while PE requires more complex approaches to rigorously represent the multi-phase transient interplay between volatile release and gaseous environment but lies outside the scope of this work. Herein, a decoupled approach is employed, where the condensed phase is simulated through a transient solver, followed by a steady-state idealized gas-phase reactor for the volatiles. A first uncertainty lies in estimating the temperature of PE and its degradation rate. The transient temperature of the polymer (T_L) is computed in analogy to the approach of Nakhaei et al. [39], employing a 0D unsteady energy balance:

$$\sum_{i\in L}\omega_i c_{p,L}^i \rho_L \frac{dT_L}{dt} = a\sigma\epsilon\left(T_{ext}^4 - T_L^4\right) + ah(T_{ext} - T_L) - \sum_j r_{L,j}\Delta h_{r_j} \quad (1)$$

where ω_i is the mass fraction of species i, $c_{p,L}^i$ its liquid-phase specific heat, a the ratio between the particle surface available for heat exchange and its volume, σ the Stefan-maxwell constant, ϵ the polymer emissivity computed as in [39], T_{ext} the gas-phase environment temperature, $r_{L,j}$ the rate of liquid-phase reaction j, and Δh_{r_j} the corresponding reaction enthalpy. In this equation, T_L represents the particle's kinetic average temperature and is analogous to a "wet bulb" temperature for polymer degradation. Experimental studies [39] have confirmed that even for $T_{ext} > 900$ °C, the temperature of PE remains below 600 °C. Coupling this equation to the polymer condensed-phase kinetic model [9] allows computing both the rate and composition of volatile release.

The secondary gas-phase reactivity is computed by assuming instantaneous mixing, idealized flow, and neglecting the unsteady behavior. Specifically, the inert mass flowrate ($\dot{m}_i$) is combined to the time-average mass flowrate of volatiles ($\dot{m}_V$) evaluated through the condensed-phase simulation. Generally, plug flow behavior is considered for the gas mixture. Most experimental studies report a nominal residence time (τ), which is usually computed based only on the normal inert volumetric flowrate. In this work, the integral residence time is computed on-the-fly according to the geometry of the experimental setup. This accounts both for the additional volatile flowrate and the variation in moles as the reaction proceeds.

This methodology relies on assumptions and simplifications suitable for lab-scale experimental setups, while industrial configurations require more advance simulation tools. Computational fluid dynamics, chemical reactor network, and residence time distribution analysis offer insight into transport and mixing phenomena, with this approach being a reliable first approximation. To assess the effect of transport limitations on model predictions, sensitivity to volatile mass flow rate $\dot{m}_V$, the most relevant output of the condensed-phase model, is analyzed, as it affects the gas-phase reactivity via inert fraction and residence time. Model-experiment comparison may also be impacted by axial and radial temperature gradients in experimental devices, though these are rarely discussed in polymer pyrolysis experiments.

4. Results

The proposed model is validated first with literature experimental data on C_5—C_7 olefins [19–21,24,25] and then with data on PE thermal degradation [40–44]. Data on short-chain olefins allows assessing the intrinsic kinetics, since fuel, experimental setups, and products are well characterized, while data on PE proves the model applicability in practical cases. Only the main comparisons are reported here, while complete validation is shown in the SM. Quantitative estimation of model-experiment deviations are performed with the Curve Matching index [45], which combines point and trend-wise approaches to provide better insights into model-experiment deviations.

Fig. 1 shows the comparison of the present work (solid lines), speciation experimental data [19–21] (marks), and the kinetic models proposed by the same authors [19–21] (dashed lines) for pyrolysis in a flow reactor at atmospheric pressure of NC_5H_{10} (black), NC_6H_{12} (red), and NC_7H_{14} (blue). The proposed model successfully describes the variation in product yields and degradation temperatures as a function of the fuel chain length. The main deviation lies in the underprediction of C_2H_4 yield at high temperatures from NC_5H_{10}, compared to the data of Cao et al. [21] but in agreement with their model and the data of Nagaraja et al. [22] under similar operating conditions (Fig. S1). Similarly, this model underestimates C_2H_4 yield from NC_7H_{14} with respect to the data and model of Cao et al. [20] in a flow reactor. However, it is in line with the experimental data of Garner et al. [25] (Fig. S2). Overall, good agreement is observed in terms of products of interest (i.e., C_1, C_2, C_3), butadiene, and benzene. Notably, the elevated CM scores highlight the predictive similarity between this model and those developed for each experimental dataset. The latter scores are marginally higher, as they represent averages from multiple models specifically calibrated to

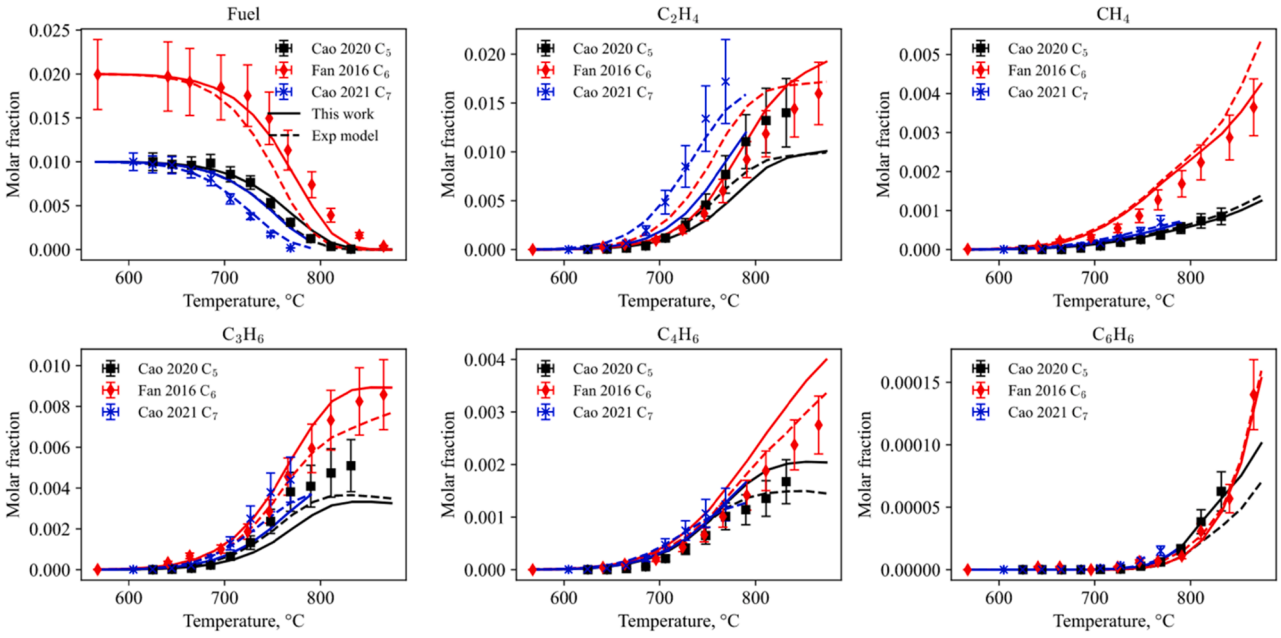

	Fuel	C_2H_4	CH_4	C_3H_6	C_4H_6	C_6H_6
This work	0.936	0.950	0.915	0.935	0.935	0.955
Exp model	0.948	0.942	0.915	0.952	0.941	0.966

Fig. 1. Outlet molar fractions in a flow reactor for NC_5H_{10} (black) [21], NC_6H_{12} (red) [19], and NC_7H_{14} (blue) [20]. Comparison of experimental data (marks), the present work (solid lines), and the models proposed by the authors' together with their experimental data (dashed lines). Average species CM scores [45] are reported in the Table below.

the respective experimental data. As mentioned, a wider validation is shown in Fig. S1-S3 including also jet-stirred and shock-tube data at different operating conditions [19–21,24,25]. The capability of the present model to reproduce experimental data as well as more detailed kinetic models demonstrates the reliability of the proposed lumping approach for modeling olefins.

To the best of the authors' knowledge, scientific literature lacks experimental data on pyrolysis of olefins longer than C_7. Further experimental data are required to validate the proposed models, although this extrapolation has already been successfully validated for alkanes steam cracking [46–48]. For this reason, the validation of the long-chain olefins model in the present work is based on PE pyrolysis data. Experimental setups with increasing complexity are presented in the following paragraphs. Two-stage reactors are privileged, as they allow investigating the secondary gas-phase reactions while reducing the variability related to condensed- phase phenomena.

Fig. 2 shows the comparison of model predictions and the data of Fu et al. [40]. The polymer is pyrolyzed in a fixed-bed setup at 500 °C and the volatiles are fed to a second reaction zone ($D = 0.4$ cm, $L = 40$ cm [49]) kept at 700–1000 °C. According to the condensed-phase model, the polymer decomposes at ~475 °C, while the volatiles are assumed to react isothermally at the nominal temperature of the second stage since no temperature profiles were reported. The authors also report the yields of the first stage, which the condensed-phase model [9] satisfactorily captures within a ~5 % relative error. The shaded area in Fig. 2 represents variation in model predictions when $\dot{m}_V$ varies by ±50 %. The rate of volatile release has a greater impact at high temperatures, where small variations in residence times are amplified by the fast kinetics. According to the present approach, while higher $\dot{m}_V$ results in higher reactant concentrations, the decrease in gas-phase residence time has a stronger impact. The left panel of Fig. 2 shows the variation in liquid and gas yields, where the model correctly captures the sharp decrease in liquid yields, due to the decomposition of C_{6+} volatiles, but also its increase at high temperatures because of condensation reactions leading

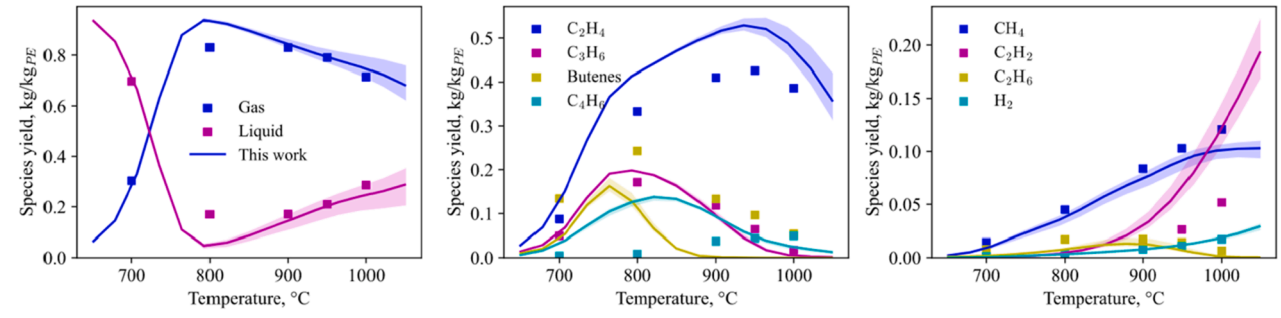

	Gas	Liquid	C_2H_4	C_3H_6	Butenes	C_4H_6	CH_4	C_2H_2	C_2H_6	H_2
This work	0.831	0.890	0.933	0.916	0.776	0.759	0.953	0.926	0.830	0.938

Fig. 2. Predicted and measured [40] species mass yield in a two-stage reactor. The shaded area represents variation in model predictions upon modifying volatiles mass flowrate ($\dot{m}_V$) by ±50 %. Average species CM scores [45] are reported below.

to the formation of mono and polyaromatic compounds. Considering the yield in short olefins (Fig. 2 center panel), the model correctly reproduces the maximum trend in ethylene, although overestimating the absolute value, while agreeing with data from Artetxe et al. [41] (Fig. S4) under similar nominal operating conditions. The model correctly captures the variation in propylene yield, while deviations are observed with respect to butenes and butadiene. C_4H_6 is not experimentally observed at low temperatures but is among the main compounds obtained from olefin pyrolysis as shown in Fig. 1. With respect to other light gases (Fig. 2 right panel), the model correctly captures CH_4, H_2, and C_2H_6, while overestimating C_2H_2 formation at high temperatures. The model shows reasonably high CM scores for most species, with lower values for global yields, ethane and C_4 compounds, where the latter shows the highest deviations with a better agreement in terms of total C_4 fraction. The lower CM scores compared to Fig. 1 may be due to the simplified simulation approach used to model PE pyrolysis, but also the intrinsic variability of polymer samples, or experimental uncertainties.

The proposed model is also validated considering data on thermal degradation of PE in a drop tube reactor [42] as shown in Fig. 3. The molten polymer is dropped inside an environment at 500–900 °C and the released volatiles react for a length of 8.3 cm or 48.86 cm. The former length is referred to as short residence time (SRT, τ=3–4 s), while the latter length is referred to as long residence time (LRT, τ=17–26 s). According to the condensed-phase model, in the current setup the polymer decomposition temperature does not increase above 550 °C even for an external environment of 900 °C, in line with literature experiments [39,50]. Higher reaction temperatures can be obtained for particles with larger surface-to-volume ratios and transport coefficients. The estimation of T_L is crucial to predict the subsequent reactivity of the volatiles, as higher temperatures significantly increase in $\dot{m}_V$, which, in turn, leads to higher reactant concentrations and shorter residence times. Consequently, following the proposed methodology, $\dot{m}_v$ has a greater effect than the composition of volatiles released. The left panel of Fig. 3 shows the comparison of model predictions and experimental results for short and long residence times in terms of cumulative carbon conversion, which corresponds to the total moles of carbon in all carbon gas products detected by a mass spectrometer (CH_4, C_2H_4, C_2H_6, C_3H_6, and C_3H_8) [42]. The model correctly captures the total molar yield of LRT (red) and the trend but not absolute values of SRT (blue), as shown by the CM scores. For the model, increasing the residence time shifts the reactivity toward a lower temperature with minor effect on product distribution. This is possibly a consequence of the simplified degradation of terminal radicals from long-chain olefins, where rate parameters at 700 °C are considered. However, this approximation has been verified to have a minor impact on modeling steam cracking reactors [34]. A more detailed look into the individual species yields is reported in Fig. 3 center panel for SRT and Fig. 3 right panel for LRT conditions. Considering SRT, the model correctly reproduces the formation of methane and hydrogen but underestimates the yields of C_3H_6 and C_2H_4 at high temperatures. The predicted ethylene yield does not exceed 40–50 wt. % coherently with the data of Fu et al. [40] (Fig. 2) and Artetxe et al. [41] (Fig. S4), predicting a decrease at higher temperatures because of condensation and dehydrogenation reactions. As previously mentioned, the model predicts LRT to have qualitatively similar profiles to SRT, although shifted at lower temperatures. Compared with these experimental data, the model correctly predicts the propylene yield across the investigated temperatures, while it overestimates the maximum yield of C_2H_4 but correctly captures its decrease at higher temperatures. Conversely, the model underestimates CH_4 yield and slightly underestimates H_2 formation at 900 °C. Overall, it satisfactorily reproduces experimental results as highlighted by the CM scores, despite significant but hardly avoidable simplifications required to model such complex physical systems.

Model predictions are investigated through sensitivity, flux and energy analyses. Fig. 4 shows the local integral sensitivity coefficients of fuel and C_2H_4, while the coefficients for C_3H_6, CH_4, and benzene, and a flux analysis at 600 and 1000 °C can be seen in the SM (Fig. S7 and S8) because of space limitations. Fuel initiations are the most sensitive reactions across all species, with alkyl initiation reactions prevailing at $T >$ 1000 °C. At $T <$ 800 °C H-abstractions and radical isomerization are influential, with C_3H_5-A, CH_3, and H being key radicals respectively at low, medium, and high T. Aromatic formation (Fig. S7f) is most sensitive to C_2H_3 formation due to its subsequent addition to C_4H_6. These findings align with the flux analysis (Fig. S8). At 600 °C, H-abstractions followed by beta-scissions progressively form smaller olefins until C_3–C_5 unsaturated compounds. Conversely, at 1000 °C initiation reactions form terminal radicals that directly release NC_6H_{12} and C_2H_4 which further decompose and evolve into aromatics over time. Similar results are observed when considering heat release analyses, where H-abstractions are the main heat-sink only at 600 °C, with initiations dominating at higher temperatures.

5. Conclusions

This work proposes a kinetic model for the gas-phase reactivity of volatiles formed during PE pyrolysis. Building on literature data on C_5–C_7 olefins, a lumped approach is proposed to model the reactivity of longer chain olefins. This lumping fails when O_2 addition to alkenyl radicals is competitive with β-scission, though it can be extended by introducing the relevant chemical species. For paraffins, which have higher low T reactivity than olefins [18], this occurs in air at $T <$ 700 °C at $P = 10$ atm [12,16], i.e., outside typical PW thermochemical recycling conditions [3]. The kinetic model, freely available on GitHub [23] and here attached as SM, is validated against literature experimental data. Initial validation with pure olefins data confirms the model's capability

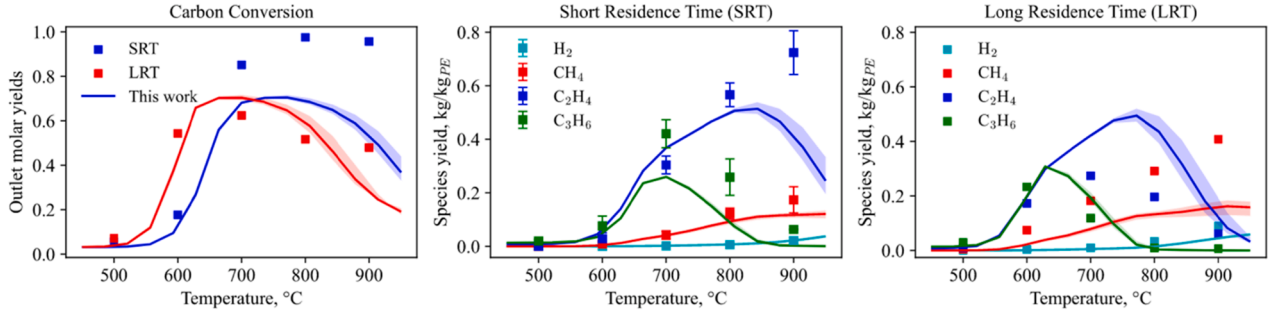

Fig. 3. Predicted and measured [42] species mass yield in a drop- tube reactor. The shaded area represents the variation in model predictions upon modifying volatiles mass flowrate ($\dot{m}_V$) by ±50 %. Average species CM scores [45] are reported below.

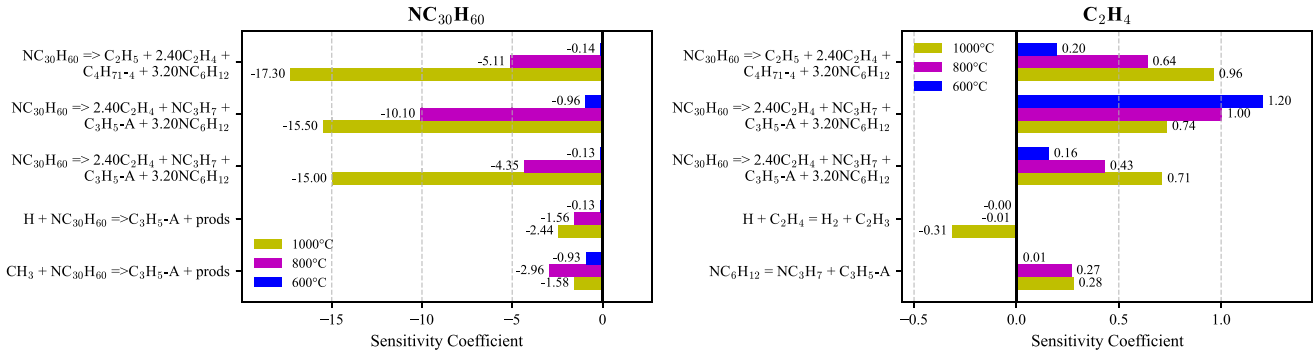

Fig. 4. Local integral sensitivity coefficients [38] in a tubular reactor at conditions analogous to Fig. 2 [40].

to reproduce both experiments and detailed kinetic models. Further experimental work is required to properly assess the proposed reactivity of long-chain olefins (i.e., $>C_7$). The overall model is employed to describe the coupling of condensed and gas-phase reactivity in PE pyrolysis. Polymer temperature is computed through a simplified energy balance, while volatiles are treated as isothermal plug flow at reactor temperature. The model aligns well with experimental results, though some deviations persist, possibly due to uncertainties in the kinetic or mathematical model, the latter being expected to have greater influence.

This work lays the groundwork for future refinement using more advanced tools such as CFD, chemical reactor network, and residence time distribution analysis. These methods enable deeper insights into the effect of polymer heat transfer, mixing of inert gases and volatiles, and residence time distributions. Overall, this represents a key first step toward understanding condensed and gas-phase interactions in waste thermochemical valorization and supports modeling of secondary degradation in other relevant polymers, including those employed for solid propellants and fire safety studies.

Novelty and significance statement

The present work proposes a comprehensive kinetic model to describe the condensed and secondary gas-phase thermal degradation of PE. The novelty of the present paper lies both in the model itself, which is the first fundamental model able to describe polymer degradation comprehensively, and the methodology itself. Building on reaction-class based approaches proposed in the scientific literature, this work employs a consistent lumped approach to model all long chain volatile released from polymer decomposition at a low computational cost. The proposed methodology is developed to enable direct coupling with detailed core models that enable describing formation of pollutants in detail. This is also the first work to quantitatively assess the coupling between the condensed and gas-phase phenomena by introducing an appropriate energy balance and evaluating its effect on the subsequent volatile reactivity. The proposed methodology is not polymer specific and can be extended to model any polymeric system, from plastic waste to solid propellants.

Disclaimer

This project was funded by the United States Department of Energy, National Energy Technology Laboratory, in part, through a site support contract. Neither the United States Government nor any agency thereof, nor any of their employees, nor the support contractor, nor any of their employees, makes any warranty, express or implied, or assumes any legal liability or responsibility for the accuracy, completeness, or usefulness of any information, apparatus, product, or process disclosed, or represents that its use would not infringe privately owned rights. Reference herein to any specific commercial product, process, or service by trade name, trademark, manufacturer, or otherwise does not necessarily constitute or imply its endorsement, recommendation, or favoring by the United States Government or any agency thereof. The views and opinions of authors expressed herein do not necessarily state or reflect those of the United States Government or any agency thereof.

CRediT authorship contribution statement

Andrea Locaspi: Conceptualization, Methodology, Investigation, Validation, Visualization, Writing – original draft. **Alessandro Pegurri:** Methodology, Investigation, Validation, Visualization, Writing – review & editing. **Marco Mehl:** Methodology, Investigation. **Matteo Pelucchi:** Methodology, Investigation, Writing – review & editing. **Sittichai Natesakhawat:** Writing – review & editing. **Hang Zhou:** Writing – review & editing. **Yupeng Xu:** Writing – review & editing. **Ping Wang:** Writing – review & editing. **Mehrdad Shahnam:** Writing – review & editing, Project administration, Funding acquisition. **Tiziano Faravelli:** Conceptualization, Writing – review & editing, Supervision, Project administration, Funding acquisition.

Declaration of competing interest

The authors declare that they have no known competing financial interests or personal relationships that could have appeared to influence the work reported in this paper.

Acknowledgements

This work was performed in support of the U.S. Department of Energy's (DOE) Office of Fossil Energy and Carbon Management's Gasification Program and executed through the National Energy Technology Laboratory (NETL) Research & Innovation Center's Advanced Reaction Systems Field Work Proposal. This project has received funding from the European Union's Horizon Europe research and innovation programme under the HORIZON—CL4-–2021-TWIN-TRANSITION-01 grant agreement No 101058412. Views and opinions expressed are however those of the author(s) only and do not necessarily reflect those of the European Union or HADEA. Neither the European Union nor the granting authority can be held responsible for them.

Supplementary materials

Supplementary material associated with this article can be found, in the online version, at doi:10.1016/j.proci.2025.105912.

References

[1] O. Dogu, M. Pelucchi, R. Van de Vijver, P.H.M. Van Steenberge, D.R. D'hooge, A. Cuoci, M. Mehl, A. Frassoldati, T. Faravelli, K.M. Van Geem, The chemistry of chemical recycling of solid plastic waste via pyrolysis and gasification: state-of-the-art, challenges, and future directions, Prog. Energy Combust. Sci. 84 (2021) 100901.

[2] U. Arena, Process and technological aspects of municipal solid waste gasification. A review, Waste Manage 32 (2012) 625–639.
[3] S. Madanikashani, L.A. Vandewalle, S. De Meester, J. De Wilde, K.M. Van Geem, Multi-scale modeling of plastic waste gasification: opportunities and challenges, Materials. (Basel) 15 (2022) 4215.
[4] R.E. Harmon, G. Sribala, L.J. Broadbelt, A.K. Burnham, Insight into polyethylene and polypropylene pyrolysis: global and mechanistic models, Energy & Fuels 35 (2021) 6765–6775.
[5] A. Locaspi, M. Ferri, F. Serse, M. Maestri, M. Pelucchi, Chemical Kinetics of Catalytic/Non-Catalytic Pyrolysis and Gasification of Solid Plastic Wastes, Academic Press, 2022.
[6] R.W.J. Westerhout, M.P. Van Koningsbruggen, A.G.J. Van Der Ham, J.A. M. Kuipers, W.P.M. Van Swaaij, Techno-economic evaluation of high temperature pyrolysis processes for mixed plastic waste, Chem. Eng. Res. Des. 76 (1998) 427–439.
[7] G. Elordi, G. Lopez, M. Olazar, R. Aguado, J. Bilbao, Product distribution modelling in the thermal pyrolysis of high density polyethylene, J. Hazard. Mater. 144 (2007) 708–714.
[8] A. Locaspi, M. Pelucchi, M. Mehl, T. Faravelli, Towards a lumped approach for solid plastic waste gasification: polyethylene and polypropylene pyrolysis, Waste Manage 156 (2022) 107–117.
[9] A. Locaspi, A. Frassoldati, T. Faravelli, Reduced-order condensed-phase kinetic models for polyethylene, polypropylene and polystyrene thermochemical recycling, Chem. Eng. J. (2024) 156949.
[10] S.E. Levine, L.J. Broadbelt, Detailed mechanistic modeling of high-density polyethylene pyrolysis: low molecular weight product evolution, Polym. Degrad. Stab. 94 (2009) 810–822.
[11] M.L. Poutsma, Reexamination of the pyrolysis of polyethylene: data needs, free-radical mechanistic considerations, and thermochemical kinetic simulation of initial product-forming pathways, Macromolecules. 36 (2003) 8931–8957.
[12] A.F. Ranzi, A. Stagni, M. Pelucchi, A. Cuoci, T. Faravelli, E. Ranzi, A. Frassoldati, A. Stagni, M. Pelucchi, A. Cuoci, T. Faravelli, A.F. Ranzi, A. Stagni, M. Pelucchi, A. Cuoci, T. Faravelli, Reduced kinetic schemes of complex reaction systems: fossil and biomass-derived transportation fuels, Int. J. Chem. Kinet. 46 (2014) 512–542.
[13] T. Buzogány, I. Amghizar, G.B. Marin, G.J. Heynderickx, K.M. Van Geem, Challenges and opportunities in process simulation for the transition from fossil to sustainable feedstocks: a steam cracking case study, Engineering (2025) under review.
[14] E. Ranzi, C. Cavallotti, A. Cuoci, A. Frassoldati, M. Pelucchi, T. Faravelli, New reaction classes in the kinetic modeling of low temperature oxidation of n-alkanes, Combust. Flame 162 (2015) 1679–1691.
[15] H.J. Curran, Developing detailed chemical kinetic mechanisms for fuel combustion, Proc. Combust. Inst. 37 (2019) 57–81.
[16] S. Dong, S.W. Wagnon, L. Pratali Maffei, G. Kukkadapu, A. Nobili, Q. Mao, M. Pelucchi, L. Cai, K. Zhang, M. Raju, T. Chatterjee, W.J. Pitz, T. Faravelli, H. Pitsch, P.K. Senecal, H.J. Curran, A new detailed kinetic model for surrogate fuels: c3MechV3.3, Appl. Energy Combust. Sci. 9 (2022) 100043.
[17] C.K. Westbrook, W.J. Pitz, O. Herbinet, H.J. Curran, E.J. Silke, A comprehensive detailed chemical kinetic reaction mechanism for combustion of n-alkane hydrocarbons from n-octane to n-hexadecane, Combust. Flame 156 (2009) 181–199.
[18] C.W. Zhou, A. Farooq, L. Yang, A.M. Mebel, Combustion chemistry of alkenes and alkadienes, Prog. Energy Combust. Sci. 90 (2022) 100983.
[19] X. Fan, G. Wang, Y. Li, Z. Wang, W. Yuan, L. Zhao, Experimental and kinetic modeling study of 1-hexene combustion at various pressures, Combust. Flame 173 (2016) 151–160.
[20] C. Cao, W. Li, Q. Xu, B. Feng, Z. Wang, J. Yang, Y. Li, Probing pyrolysis chemistry of 1-heptene pyrolysis with insight into fuel molecular structure effects, Combust. Flame 227 (2021) 79–94.
[21] C. Cao, W. Li, W. Chen, H. Ahmad, J. Yang, Y. Li, Exploring combustion chemistry of 1-pentene: flow reactor pyrolysis at various pressures and development of a detailed combustion model, Int. J. Chem. Kinet. 53 (2021) 514–526.
[22] S.S. Nagaraja, J. Power, G. Kukkadapu, S. Dong, S.W. Wagnon, W.J. Pitz, H. J. Curran, A single pulse shock tube study of pentene isomer pyrolysis, Proc. Combust. Inst. 38 (2021) 881–889.
[23] CRECK Modeling Lab, Kinetic-mechanisms, accessed August 2025, https://github.com/CRECKMODELING/Kinetic-Mechanisms.
[24] S.S. Nagaraja, J. Liang, S. Dong, S. Panigrahy, A. Sahu, G. Kukkadapu, S. W. Wagnon, W.J. Pitz, H.J. Curran, A hierarchical single-pulse shock tube pyrolysis study of C2–C6 1-alkenes, Combust. Flame 219 (2020) 456–466.
[25] S. Garner, R. Sivaramakrishnan, K. Brezinsky, The high-pressure pyrolysis of saturated and unsaturated C7 hydrocarbons, Proc. Combust. Inst. 32 (2009) 461–467.
[26] E. Ranzi, M. Dente, A. Goldaniga, G. Bozzano, T. Faravelli, Lumping procedures in detailed kinetic modeling of gasification, pyrolysis, partial oxidation and combustion of hydrocarbon mixtures, Prog. Energy Combust. Sci. 27 (2001) 99–139.
[27] L.T. Creadore, A. Locaspi, T.M. Marchese, M. Pelucchi, T. Faravelli, M.J. Castaldi, A semi-detailed chemical kinetic model of polybutadiene pyrolysis, Fuel 405 (2026) 136572.
[28] A. Locaspi, O. Akin, D. Withoeck, M. Havaei, A. Frassoldati, L.P. Maffei, M. Pelucchi, M. Mehl, R.J. Varghese, K.M. Van Geem, T. Faravelli, A lumped kinetic model and experimental investigation of poly(ethylene terephthalate) condensed-phase pyrolysis, Chem. Eng. J. 500 (2024) 156955.
[29] A.T. Holley, X.Q. You, E. Dames, H. Wang, F.N. Egolfopoulos, Sensitivity of propagation and extinction of large hydrocarbon flames to fuel diffusion, Proc. Combust. Inst. 32 (2009) 1157–1163.
[30] Y. Nannoolal, J. Rarey, D. Ramjugernath, Estimation of pure component properties: part 2. Estimation of critical property data by group contribution, Fluid. Phase Equilib. 252 (2007) 1–27.
[31] G. Bagheri, E. Ranzi, M. Pelucchi, A. Parente, A. Frassoldati, T. Faravelli, Comprehensive kinetic study of combustion technologies for low environmental impact: MILD and OXY-fuel combustion of methane, Combust. Flame 212 (2020) 142–155.
[32] A. Nobili, A. Cuoci, W. Pejpichestakul, M. Pelucchi, C. Cavallotti, T. Faravelli, Modeling soot particles as stable radicals: a chemical kinetic study on formation and oxidation. Part I. Soot formation in ethylene laminar premixed and counterflow diffusion flames, Combust. Flame 243 (2022) 112073.
[33] E. Ranzi, M. Dente, S. Pieruccl, G. Blardl, Initial product distributions from pyrolysis of normal and branched paraffins, Ind. Eng. Chem. Fundam. 22 (1983) 132–139.
[34] M. Dente, G. Bozzano, T. Faravelli, A. Marongiu, S. Pierucci, E. Ranzi, Kinetic modelling of pyrolysis processes in gas and condensed phase, Adv. Chem. Eng. 32 (2007) 51–166.
[35] M. Mehl, G. Vanhove, W.J. Pitz, E. Ranzi, Oxidation and combustion of the n-hexene isomers: a wide range kinetic modeling study, Combust. Flame 155 (2008) 756–772.
[36] P.J. Linstrom, W.G. Mallard, The NIST chemistry WebBook: a chemical data resource on the internet†, J. Chem. Eng. Data 46 (2001) 1059–1063.
[37] G. Popelier, F. Vermeire, M. Djokic, R. De Bruycker, M. Sabbe, K.M. Van Geem, Steam cracking of methyl ester: a modeling study on the influence of the hydrocarbon backbone, J. Anal. Appl. Pyrolysis. 172 (2023) 105998.
[38] A. Cuoci, A. Frassoldati, T. Faravelli, E. Ranzi, OpenSMOKE++: an object-oriented framework for the numerical modeling of reactive systems with detailed kinetic mechanisms, Comput. Phys. Commun. 192 (2015) 237–264.
[39] M. Nakhaei, H. Wu, D. Grévain, L.S. Jensen, P. Glarborg, S. Clausen, K. Dam-Johansen, Experiments and modeling of single plastic particle conversion in suspension, Fuel Process. Technol. 178 (2018) 213–225.
[40] Z. Fu, F. Hua, S. Yang, H. Wang, Y. Cheng, Evolution of light olefins during the pyrolysis of polyethylene in a two-stage process, J. Anal. Appl. Pyrolysis. 169 (2023) 105877.
[41] M. Artetxe, G. Lopez, M. Amutio, J. Bilbao, M. Olazar, Kinetic modelling of the cracking of HDPE pyrolysis volatiles on a HZSM-5 zeolite based catalyst, Chem. Eng. Sci. 116 (2014) 635–644.
[42] S. Natesakhawat, J. Weidman, S. Garcia, N.C. Means, P. Wang, Pyrolysis of high-density polyethylene: degradation behaviors, kinetics, and product characteristics, J. Energy Inst. 116 (2024) 101738.
[43] V. Cozzani, C. Nicolella, M. Rovatti, L. Tognotti, Influence of gas-phase reactions on the product yields obtained in the pyrolysis of polyethylene, Ind. Eng. Chem. Res. 36 (1997) 342–348.
[44] M. Della Zassa, M. Favero, P. Canu, Two-steps selective thermal depolymerization of polyethylene. 1: feasibility and effect of devolatilization heating policy, J. Anal. Appl. Pyrolysis. 87 (2010) 248–255.
[45] E. Ramalli, T. Dinelli, A. Nobili, A. Stagni, B. Pernici, T. Faravelli, Automatic validation and analysis of predictive models by means of big data and data science, Chem. Eng. J. 454 (2023) 140149.
[46] M. Dente, E. Ranzi, A.G. Goossens, Detailed prediction of olefin yields from hydrocarbon pyrolysis through a fundamental simulation model (SPYRO), Comput. Chem. Eng. 3 (1979) 61–75.
[47] P.J. Clymans, G.F. Froment, Computer-generation of reaction paths and rate equations in the thermal cracking of normal and branched paraffins, Comput. Chem. Eng. 8 (1984) 137–142.
[48] E. Ranzi, A. Frassoldati, S. Granata, T. Faravelli, Wide-range kinetic modeling study of the pyrolysis, partial oxidation, and combustion of heavy n-alkanes, Ind. Eng. Chem. Res. 44 (2005) 5170–5183.
[49] Q. Sun, Y. Cheng, Private communication, (2024).
[50] T. Kashiwagi, T.J. Ohlemiller, A study of oxygen effects on nonflaming transient gasification of PMMA and PE during thermal irradiation, Symp. Combust. 19 (1982) 815–823.